05/03/06

Superstructural Units in Borate Glasses

JANE DOUGLAS

ABSTRACT

1.~~1.~~ INTRODUCTION

Whilst crystals have long range order, and glasses are conventionally considered to have only short range order, borate glasses appear to have *medium range* order resulting from the superstructural units within the glass structure. It is the presence of these distinctive units which makes borate glass structure a particularly interesting subject for investigation.

The borate superstructural units are arrangements of linked boron and oxygen atoms: specifically arrangements of the basic 3-coordinated BO_3 (triangular) and 4-coordinated BO_4 (tetrahedral) units. Characterizing and quantifying these units is a task of importance because the superstructural unit content, which varies with the composition of the glass, contributes to the physical properties of the glass itself. The physical properties of the glass of course determine what practical applications it may be used for: sequestering radioactive waste, for example.

NMR spectroscopy is one means ~~with~~ by which superstructural unit content may be determined; Raman spectroscopy is another. NMR spectra quantitatively indicate the amount of 3- and 4-coordinated boron present. Raman spectroscopy indicates the presence and relative amounts of superstructural units, whose proportions of 4-coordinated boron can be calculated, but is not quantitative. Whilst Raman spectroscopy is not currently quantitative, it has the advantage over NMR of being insensitive to the magnetic susceptibility of the sample under consideration. This advantage becomes important in, for instance, the case of glasses produced in the vitrification of nuclear waste, since such glasses will tend to contain paramagnetic species.

1.2. Literature Survey

In 1932, Zachariasen[1] proposed the random network theory of glasses, derived from structural principles found in crystallography. In a similar manner, Wright, Vedischeva and Shakhmatkin[2] consider the crystal structure of anhydrous borates and infer a structural theory for borate glasses.

The fraction of 4-coordinated boron atoms, N4, in borate glasses is very interesting to those examining borate glass structure: Hannon and Holland[3] put forward a parameterisation for the composition-dependence of N4, in borate glasses, and Jellison, Feller and Bray[4] also contribute to the discussion of N4 (specifically in lithium borate glasses).

NMR is often used as the chief method of investigation into borate glass structure, such as in the examination by Kroeker et al.[5] of medium range order in caesium borate glasses. Wüllen and Müller-Warmuth[6] discuss the use of magic-angle spinning (MAS) NMR spectroscopy for probing glass structures.

Medek and Frydman[7] introduced multiple-quantum magic-angle spinning (MQMAS) NMR as a new experimental tool for investigating quadrupolar nuclei. Brown and Wimperis[8] actually employed 2D MQMAS to examine quadrupolar nuclei in a method that will be relevant to later work in this study. Stebbins, Zhao and Kroeker[9] employed both ^{11}B MAS and triple-quantum MAS NMR to characterize the non-bridging oxygens in borate glasses.

Raman provides another means with which to investigate borate glass structures. Meera and Ramakrishna[10] comprehensively cover the subject in their paper, and Dwivedi et al.[11] have carried out a Raman study of lithium borate glasses (our specific glass of interest). The identification of superstructural groups by attributing particular units, and unit breathing modes, to particular Raman spectra peaks will be achieved via a thorough survey of the peak assignments proposed by the two studies above, as well as the studies of Kamitsos et al.[12], Konijnendijk and Stevels[13].

Neutron diffraction is a third method that is useful in the probing borate glass structure, as in the work of Shaw et al.[14], though this technique is not employed in this study.

2. GLASSES AND SUPERSTRUCTURAL UNITS

2.1. Glass structure

The atoms of glasses, like those of crystals, form extended three-dimensional networks. However, whilst in crystals these networks are periodic and symmetric, that is, have *long range* order, in a glass there is an 'infinite' unit cell in which no two atoms are structurally equivalent. The atomic network of a glass is conventionally considered to be determined by Zachariasen's[1] random network theory, which proposes that a glass network is composed of small structural units 'randomly' linked in a three-dimensional arrangement. Such a network, however, has *short range* order only.

By first considering simple oxide glasses, such as those formed by individual oxides like SiO_2 and B_2O_3 (of general form A_mO_n), Zachariasen suggests that in these glass networks there are polyhedra of oxygen atoms around the A atoms. Zachariasen

goes on to extrapolate for oxide glasses in general; he maintains that a vitreous network can be built up of oxygen tetrahedra or oxygen triangles centred around the A atoms. These polyhedra must have only corners in common in order to prevent them from lining up regularly (and thus producing a crystal-like structure), and an oxygen atom must not be shared by more than two of these polyhedra.

Zachariasen also notes that in an oxygen triangle, a boron atom will, significantly, lie flat in the plane of the shape, whilst in a similar arrangement other atoms would be found displaced out of the plane; he deduces that B_2O_3 should form glass with greater ease than any other oxide.

It is borate glass with which this study is particularly concerned. Vitreous B_2O_3 is an excellent glass former, producing binary glasses with many other oxides. The glass specifically under consideration here is $xLi_2O.(100\text{-}x)B_2O_3$, where x is molar percentage. Of the various $M_2O\text{-}B_2O_3$ glass systems, the lithium borate system has a large glass-forming region: that is, a large range of x values over which glasses can be generated.

2.2. Superstructural units in borate glasses

In their paper, Wright et al.[2] provide a structural model which allows us to predict the fraction of 4-coordinated boron atoms, N4, in vitreous borate networks. Generally, the components of a glass are classed as 'network formers' and 'network modifiers', where the former contribute to the basic three-dimensional network and the latter lead to the formation of non-bridging oxygen atoms.

In the case of B_2O_3 however, the addition of a modifier mainly causes BO_3 triangles to be converted into BO_4; here it acts as a 'network strengthener' by increasing the boron-oxygen coordination number. As the modifier concentration increases, the fraction of 4-coordinated boron increases to a maximum and then decreases. As noted by Wright et al., the great variety of borate structural chemistry is due to the energy needed to convert BO_3 triangles into BO_4 tetrahedra being close to the energy needed to break B-O-B bridges and form non-bridging oxygens.

For our purposes, Zachariasen's random network theory alone is not sufficient to create a model of a borate glass since it neglects the superstructural units which are so distinctive. These units consist of certain configurations of the basic BO_3 and BO_4 units joined with no internal degrees of freedom or torsion angles.

The proximity of the equilibrium B-O-B bond angle to that of planar three-membered rings is an important factor bringing about superstructural units in borate glasses; the proximity leads to a favourable formation energy for superstructural units. In a system of BO_3 and BO_4 units, four 6-membered rings are possible. Larger superstructural units are formed by combining two of these rings via sharing one or two BO_4 tetrahedra (see figure 2).

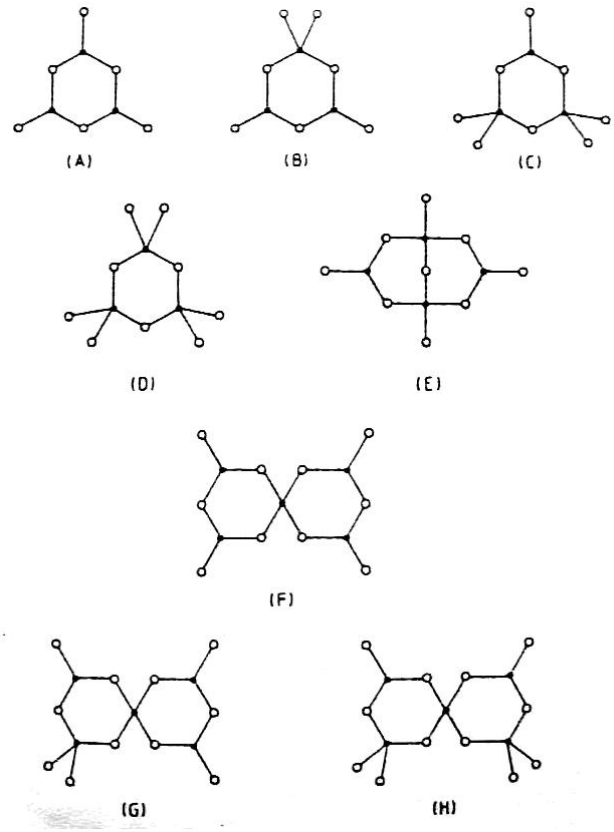

Fig. 1. Superstructural borate glass units: three-membered rings and pairs of such rings joined by one or two shared BO_4 tetrahedra.[2]

(A) boroxol group, B_3O_6 / cyclic metaborate anion $B_3O_6^{3-}$

(B) triborate group, B_3O_7

(C) di-triborate group, B_3O_8

(D) metaborate group, B_3O_9

(E) diborate group, B_4O_9

(F) pentaborate group, B_5O_{10}

(G) di-pentaborate group, B_5O_{11}

(H) tri-pentaborate group, B_5O_{12}

Following the above, the now generally accepted model for borate glasses resembles Zachariasen's 'random network', but with superstructural units connected randomly to each other, along with the smaller loose BO_3 and BO_4 units. This model introduces the *medium range* order which interests us.

2.3. Bridging and Non-Bridging Oxygen Atoms

Bridging oxygens (BOs) in a glass network are defined as oxygen atoms which link two network cations: in the case of borate glasses, the B^{3+} ion. Non-bridging oxygens (NBOs) are oxygen atoms which are attached to only one network cation.

As noted by Stebbins et al.[9], the ratio of NBOs to BOs is an important factor determining the physical properties of the glass and of the melt used to produce the glass. NBOs make the melt less viscous, and increase the susceptibility of the glass to corrosion by water. Conversely, BOs tend to lead to harder glasses that can be utilized at higher temperatures; accordingly, these glasses require higher temperatures to be melted and worked. Proportions of BOs and NBOs are therefore of interest to those considering the physical properties and practical uses of borate glasses.

2.3. The Four-Coordinated Boron Fraction

The considerations above led Wright et al. to a simple model for predicting in borate glasses the fraction of 4-coordinated boron as it varies with composition. Their model relies on three assumptions:

i. The borate network contains the maximum number of BO_4 tetrahedra allowed by the other assumptions. The BO_4^- unit in a network of BO_3 triangles has a lower formation energy than that of a BO_3 triangle with an NBO (that is, a BO_2O^- unit).
ii. There are no $B^{[4]}$-O-$B^{[4]}$ bridges.

iii. There are no BO_4 tetrahedra with NBOs.

The predictions of the model compared to experimental data from NMR spectroscopy for a Li_2O-B_2O_3 system are shown in figure 3. Below $x = 30$ (region A in the figure), the structure contains BO_3 and BO_4^- units only and N4 is predicted by:

$$N_4 = \frac{x}{(1-x)} \qquad (1)$$

At $x = 30$, we find an alternating network of the BO_3 and BO_4^- units; after this point (region B in the figure), adding further network modifier (Li_2O) causes BO_2O^- units to form until $x = 50$, where there is an alternating network of BO_4^- and and BO_2O^- units.

There is a discrepancy between the model and the data where the data forms a smooth curve without the predicted discontinuity at $x = 30$. This is a result of the perfect network of alternating BO_3 and BO_4^- (meaning rings of *even* numbers of units) being inaccessible via conventional quenching methods. The actual network will contain rings of *odd* numbers of units, which must avoid $B^{[4]}$-O-$B^{[4]}$ bridges by forming BO_2O^- units, reducing N4 up to $x = 30$.

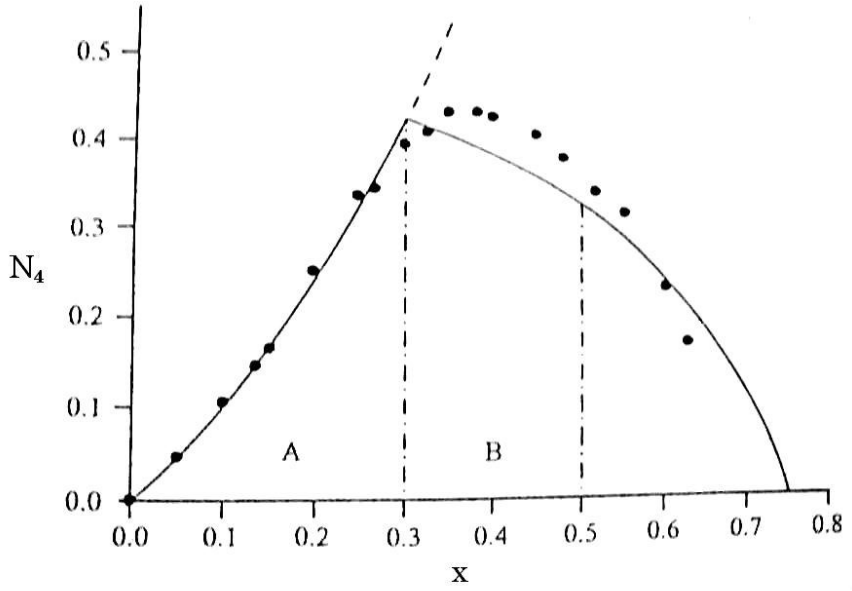

Fig. 2.

A simplified representation of the model devised by Wright et al. for predicting N4 against x for lithium borate glasses; NMR data represented by dots and the model predictions by the solid line.[2]

Some $B^{[4]}$-O-$B^{[4]}$ bridges are likely to occur as part of superstructural units which are based on rings of odd numbers of member units, especially around $x = 33.33$, the diborate composition. Here N4 is increased, explaining the data falling slightly above the line given by the model.

3. BORON-11 NMR AND MQMAS NMR

3.1. Magic Angle Spinning NMR

NMR spectroscopy probes a sample by exploiting the magnetic properties of the nuclei within. In the presence of a magnetic field, NMR-active nuclei (that is, nuclei with non-zero spin) resonate at specific frequencies; different nuclei will resonate at different frequencies according to their local environment. These nuclei

are perturbed with an radiofrequency electromagnetic field, and their response provides the signal from which information about the nuclei is extracted.

The resonant frequency will vary with magnetic field strength. It is therefore translated into a value which is independent of field strength, called chemical shift, which is the difference between the resonant frequency of a certain nucleus and that of a standard reference nucleus. Nuclei will have different chemical shifts according to their environment, and so peaks in the resulting spectra can be assigned to particular atoms, or atomic groups. The integrated area under such peaks is a reflection of the quantity of such nuclei present in the sample.

Boron-11 NMR specifically exploits the 3/2 spin of the ^{11}B atom; such a spin fulfils the non-zero criterion required for NMR spectroscopy to work. Borate glasses have been investigated for many years by means of such NMR, via low-field static spectroscopy at first (such as in the work of Jellison et al.[4]), then later with spinning samples. This technique indicates the quantities of 3- and 4-coordinated boron present in the sample.

Magic angle spinning (MAS), in which the sample is spun at an angle of 54.74°, has significantly enhanced NMR spectroscopy as a means for probing borate glass structure, as found for example in the work of Wüllen and Müller-Warmuth[6]. The spinning of the sample mimics the behaviour of isotropic molecular motion; the effect is to narrow the broad peaks of non-MAS spectra into narrow lines with spinning sidebands, whose spacing is determined by the rotational frequency.

3.2. Multiple Quantum Magic Angle Spinning

Boron-11, with a spin of 3/2, is a termed a *quadrupolar nucleus* in virtue of its electric quadrupole moment which interacts with the electric field gradient surrounding it. This quadrupolar interaction can be so strong as to overpower all but the central (-1/2 ⇔ +1/2) transitions, and even this signal is affected by second-order quadrupole effects. As discussed by Brown and Wimperis[8], multiple-quantum magic angle spinning (MQMAS) has recently become a popular NMR method for studying quadrupolar nuclei, removing the second-order quadrupolar broadening of the central transition.

MQMAS is an 2D echo experiment concerning the transitions between *non-consecutive* energy levels which take place during the excitation of the spin system by a first pulse. A second pulse converts the multiple quantum coherences thus produced back into single quantum coherences as an echo and antiecho. Medek and Frydman's paper[7] gives a comprehensive, mathematical treatment of the theoretical background of MQMAS experiments. Though now widely used, the MQMAS technique can involve problems of poor sensitivity.

These experiments make it possible to resolve inequivalent chemical sites for quadrupolar nuclei. With this technique, combined with MAS, we can also quantify the relative proportions of different chemical species present in the sample structure.

4. RAMAN SPECTROSCOPY

Convincing but non-quantitative evidence for superstructural units can be obtained using optical spectroscopy. In the case of this study, Raman spectroscopy is used to examine the vibrational modes present in the borate glass system; at room

temperature, the relevant vibrational modes are the 'breathing modes' of the structural units.

This method, wherein a sample is exposed to laser light and the resulting scattered light measured, makes use of the Raman effect. Whilst most light will be elastically scattered and therefore its energy unaltered, some light will be subject to the Raman effect which causes, upon scattering, an increase or decrease in the frequency of the incident light.

Raman spectra of borate glasses show sharp lines around 806 and 770cm^{-1}, brought about by the boroxol and triborate structural groups (A and B in figure 2) respectively. The intensity of Raman lines is proportional to the number of scattering centres and their scattering efficiency, that is, their Raman cross-section.

5. EXPERIMENTAL DETAILS

5.1. Glass making

Initially, ten $xLi_2O.(100-x)B_2O_3$ glass samples were prepared, with x ranging from 0 to 40 mol %. Li_2CO_3 and B_2O_3 powders, plus 0.1 mol % of the paramagnetic salt Fe_2O_3 to reduce relaxation time for the NMR experiments, were mixed in appropriate quantities to produce 30g batches. These were heated in large platinum-rhodium crucibles at a rate of 600°C per hour up to 1000°C, and then held at this temperature for 20 minutes. The samples were then quenched on a room-temperature, graphite-coated steel plate. After it became apparent that a heating rate as high as 600°C may have caused cross-contamination between melts (two were furnaced at a time), the final two samples, x = 35 and 40 mol % were heated at the lower rate of 300°C per hour. To avoid contamination by water, the samples were stored in a desiccator.

Simultaneous thermal analysis was employed to find the T_g of the glass samples; by comparing these T_g values to previously reported values[15], they can be used to check that the compositions of the glasses produced are correct, and how far any possible cross-contamination has affected them. A Perkin Elmer Pyris Diamond TG/DTA was used to collect the readings from which T_g values were extracted.

The second set of glass samples, a lithium borate glass doped with paramagnetic ions, of the family $xCoO.yLi_2O.zB_2O_3$, was also prepared. Li_2CO_3 and B_2O_3 were again used, plus $CoCO_3$ powder, with x ranging between 0.1 and 5 mol %, and x+y = 20 mol %. The paramagnetic species was Co^{2+}. The mixtures were again melted in platinum crucibles; they were heated at 300°C per hour up to 1000°C and held there for 20 minutes before plate quenching.

X-ray diffraction was employed to analyse a selection of the glasses, to ensure we had created glasses rather than crystals; the diffraction patterns showed broad humps rather than the sharp peaks which would have indicated crystallisation had occurred.

5.2. NMR

5.2.1. NMR spectra acquisition

The lithium borate glasses were ground into powder, and the powders were analysed with ^{11}B MAS NMR, using a CMX 600 Spectrometer tuned to 192.5MHz

and a Varian 4mm MAS probe (#6300). Boron phosphate BPO_4 was used as a secondary reference as it is known to resonate at -3.3ppm with respect to the primary reference $BF_3{:}Et_2O$.

After tuning the probe, and spinning the powdered sample up to about 10kHz, an NMR spectrum was obtained with a one-pulse experiment. A pulse delay array sequence was performed on the x = 40 sample, suggesting an appropriate pulse delay of 0.1s, being 5 times the spin lattice relaxation time T_1. Consequently, the one-pulse experiments were run with a 0.1s delay between pulses and a pulse length of 0.6μs, taking 2048 acquisitions per run.

The glasses doped with cobalt oxide were also powdered and subjected to similar one-pulse experiments, this time in a Varian T3 probe. A pulse delay array sequence was again used to check that there is sufficient time between pulses for the bulk magnetisation to return to equilibrium. The sample with the least cobalt oxide content, that is, the least paramagnetic ions, will have the longest relaxation time, and as such needs the longest pulse delay. The pulse delay array was therefore run on the 0.1 mol % paramagnetic-doped glass. This suggested a 0.2s pulse delay as suitable. The pulse length was 0.6μs again, and 1024 acquisitions were taken.

5.2.2. NMR spectra peak-fitting

In each spectrum~~a~~, a broad peak and a sharper peak were present. The former is associated with trigonal borons (B3) and the latter with tetrahedral borons (B4). The peak-fitting program DMFit[16] was used to fit these peaks. The peak property of primary interest in this case was the integrated area of the sharp peak relative to that of the broader peak within a single spectrum, as this indicates the proportion of 4-coordinated boron present in the glass.

The broad peak, attributed to the amount of 3-coordinated boron atoms, was fitted with two quadrupolar ~~curves~~lineshapes. The polarized peak, resulting from the presence of 4-coordinated boron, was fitted with two Gaussian ~~curves~~lineshapes. In the case of the lithium borate glasses containing no cobalt oxide, peak-fitting allows the area under the curves to be found and therefore a plot of 4-coordinated boron content against composition to be made. The area under the B3 peak was increased by 4%, following the recommendation of Mackenzie and Smith[17], to allow for intensity distributed in the sidebands.

In the case of the glasses with quantities of cobalt oxide added, the peaks in the NMR spectra are seen to ~~significantly~~ broaden significantly as the increasing concentrations of paramagnetic ions render NMR methods ineffective. Fitting the peaks from these glasses (which, in the absence of paramagnetic ions should have produced near-identical spectra) therefore does not yield useful data concerning the N4 fraction; it does, however, give an impression of how severely the presence of paramagnetic ion concentrations upset the NMR results.

5.2.3. MQMAS NMR

Multiple (triple) quantum MAS experiments were also attempted with certain lithium borate glass samples, and some difficulties were encountered in trying to produce the 2D spectra intended. Credit for assistance with the MQMAS experiments goes to Dr Ivan Hung of the University of Warwick.

Initially using the x = 0 mol % glass, a pre-existing MQMAS sequence was implemented for the nucleus in question. The sequence, following the phase-modulated split-t1 method established by Brown and Wimperis[8], comprises three pulses. A first pulse excites the spin system; multiple quantum coherences result, which are converted back into single quantum coherences by the second pulse; the third pulse is a selective π pulse for the central transition. Such a sequence divides the t1 evolution period between multiple and single quantum precession. This brings about the refocusing of the second order quadrupolar broadening by the end of t1. During the acquisition time, the whole echo is captured by means of shifting the echo by period τ.

The lengths of these three pulses (excitation, conversion and spin echo) were chosen by means of an optimisation pulse array, which suggested as appropriate pulse lengths of 6, 2.3 and 11.2 μs and respectively. The sample was spun at 10kHz, and the experiment was run for several hours. MQMAS results should reveal, after proper processing, two peaks in the 2D spectrum, these indicating B3 in a ring, and B3 not in a ring.

Another MQMAS experiment was attempted, this with the x = 20 mol % lithium borate glass. An optimisation pulse array this time suggested excitation, conversion and spin-echo pulse lengths of 8, 3.25 and 12.5 μs respectively. Again, the experiment was run over several hours but this time it yielded a much noisier spectrum. Processing this in appropriate way to yield interesting results proved very difficult.

5.3. Raman

5.3.1 Raman spectra acquisition

Solid, flat fragments of the lithium borate glasses were analysed with Raman spectroscopy, using a Renishaw inVia machine with a 515.4nm laser wavelength and x50 magnification. The wavenumber range was from 100 up to 3200cm^{-1}, with 50 acquisitions taken for each spectrum.*

5.3.2 Raman spectra peak-fitting

The background noise for the Raman spectra being significant, a suitable baseline subtraction was vital. This subtraction was carried out in Origin, with a second-order polynomial baseline giving the best results.

The peak-fitting for the Raman spectra was significantly more complicated than that of the NMR spectra. Originally, the peak-fitting was attempted in the DMFit program; after it became apparent that the program was unsuitable in this situation, Origin was used instead.

DMFit was inappropriate for Raman peak-fitting, at least in the case of these experiments, because it appears to take the start and end point of the 'x' value of the data set (wavenumbers, in this case) and divide this range by the number of 'y' (intensity) data points present to find an x-value interval, with which it accordingly plots the y-value data. Rather than producing a pure scatter plot of the data, DMFit assumes that the experimental data has been read at exactly regular intervals: true in the case of the NMR spectrum data, but not for the Raman readings.

* Raman readings were taken by Ben Parkinson, University of Warwick.

The primary difficulty with the Raman peak-fitting is the ambiguous nature of any peak-fit found; many alternative solutions, each with a comparably good fit to the actual data, can be obtained. With reference to the literature[10,12,13] and intuition of 'realistic' solutions, an appropriate fit was found. It is worth noting, however, that my lab partner obtained another 'appropriate' fit by similar means, and there is some discrepancy between them. This discrepancy can be used to estimate the error (in Raman peak areas) arising from ambiguity in the peak-fitting.

6. RESULTS

6.1. STA

The STA plots acquired for selected glasses was analysed to provide T_g values for the glasses in question; at the glass transition region (as opposed to the later crystal transition region), the steepest gradient of the slope was taken, and the point at which it intercepted the 'baseline' (see fig. 3). These T_g values were compared with those in the literature[15]. Since T_g is dependent on the glass composition, such a comparison reflects how closely our sample compositions match their intended compositions.

Two of the STA plots produced T_g values which were patently spurious, since they implied compositions very different from those intended; had our actual x values been this far (at least 5 mol %) from the indended x values, the NMR spectra would not have shown the regular trend that they did.

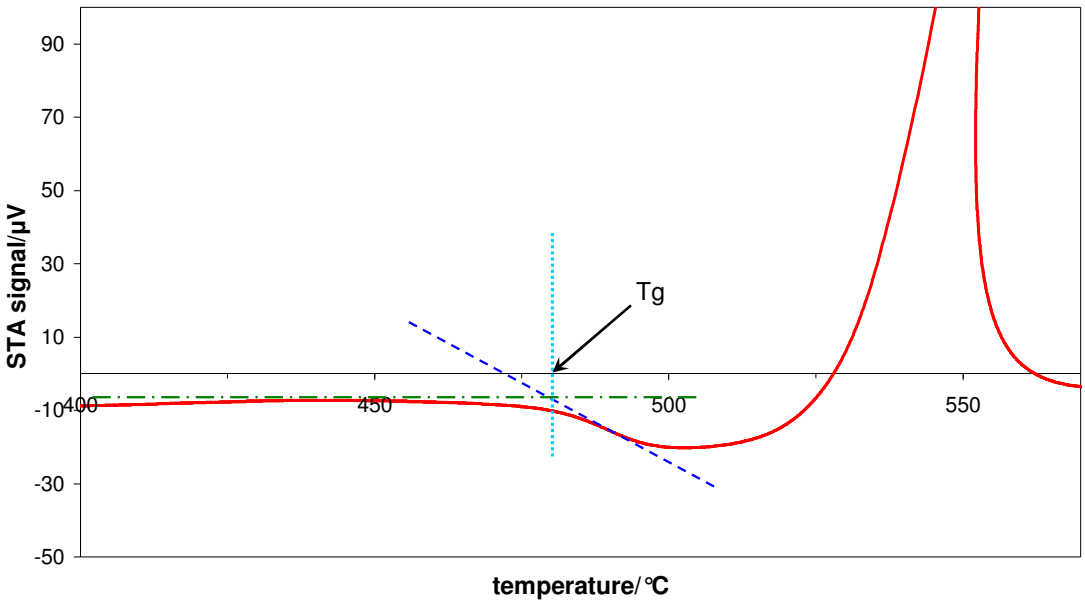

Fig. 3.

A sample STA plot (from the x = 40 mol % glass), showing how T_g was calculated. The dashed line is the steepest gradient of the transition, the dash-dot line is the 'baseline', and their intercept is read off the x-axis by the dotted line.

The remaining T_g values show discrepancies with literature values of between 2 and 6°C, which is acceptable. An estimated error of 2 mol % was thus attached to our composition values.

6.2. NMR

Fig. 4 shows the NMR spectra from lithium borate glasses, with the broad peaks on the left side indicating B3 and the sharper peaks on the left indicating B4. These peaks were fitted as described above in section 5.2.2. and integrated areas

calculated; these areas give the relative quantities of B3 and B4. N4 fraction is then given by:

$$N4 = \frac{B4}{B3 + B4}, \qquad (2)$$

which can then be plotted against composition (see fig. 5). The uncertainty in composition is a reflection of the discrepancy between T_g values, as described above. The uncertainty in N4 fraction is estimated according to the NMR data resolution and the quality of the peak fitting; the NMR data resolution is high, and uncertainty arising from it is negligible compared to that arising from the peak fitting. The NMR peak fit was a good match for the data, and was much less ambiguous than that of the Raman spectra (see 5.3.2): error was therefore estimated to be 2%.

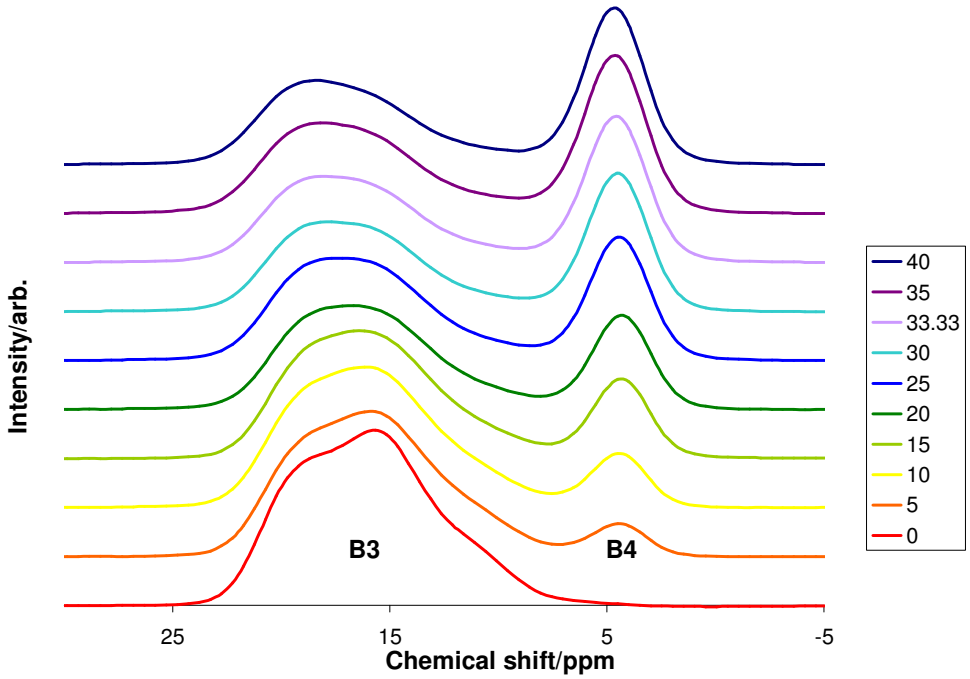

Fig. 4.

A stacked plot of the NMR spectra, with one line for each of the lithium borate glasses. Heights are not to be quantitatively compared; it is area under peaks that is of significance. The peaks on the left relate to the quantity of 3-coordinated boron, the peaks on the right to 4-coordinated boron.

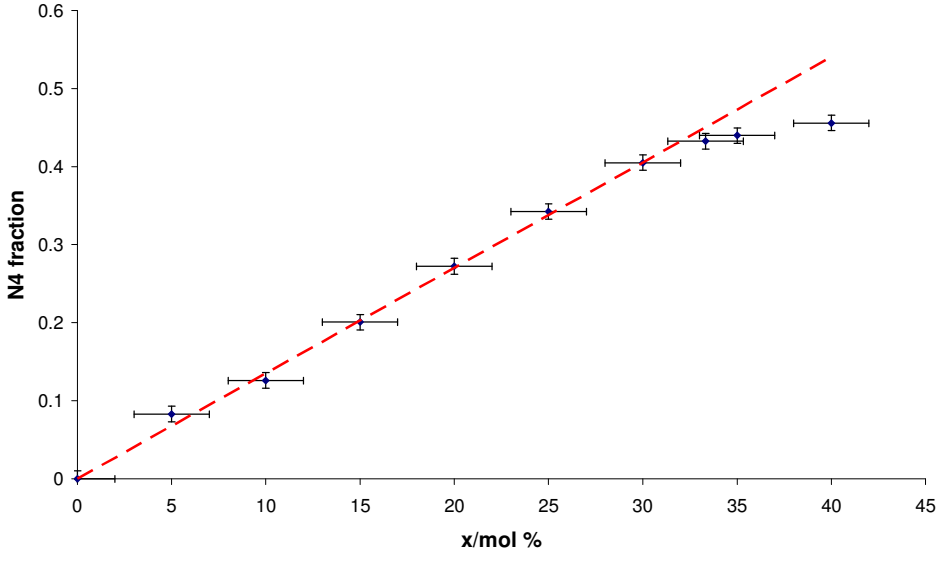

Fig. 5.

N4, the fraction of 4-coordinated boron, against composition for the lithium borate glasses. A straight line fits x = 0 to 30 very well; after x = 30, the data points curve away, reaching a plateau or turning point. This compares well with the Wright et al.'s N4 model (see fig. 2).

The glasses doped with paramagnetic ions gave the NMR spectra in fig. 6. It can be clearly seen how the Co^{2+} ions render the NMR method ineffective due to its sensitivity to magnetic susceptibility, broadening the two peaks significantly from 0.5 mol % onwards, so that by 5 mol % they are completely indistinguishable. Since the molar quantities of the lithium and boron species are basically unaltered, the NMR spectra should have been nearly identical if NMR were unaffected by magnetic susceptibility. It is this effect that means Raman spectroscopy (or another magnetism-insensitive method) is required to study the structure of such glasses.

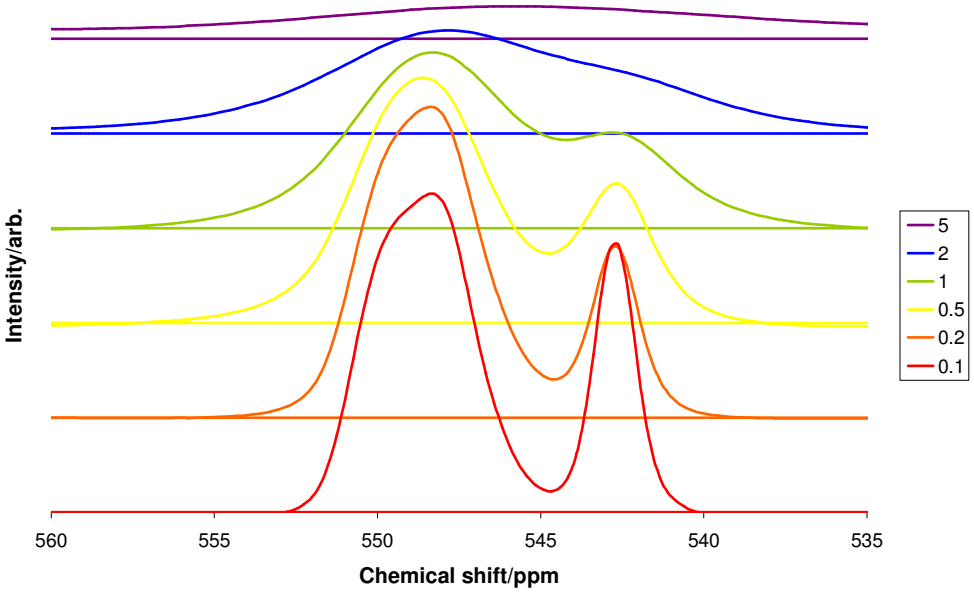

Fig. 6.

A stacked plot of the NMR spectra, with one line for each of the lithium borate glasses doped with cobalt oxide.

After suitable processing, the first MQMAS experiment (for the x = 0 mol % borate glass) produced the 2D spectrum seen in fig. 6. The black areas on the plot represent positive values, that is, peaks, whilst the red areas represent negative values ('valleys'). Noise has been largely removed via processing.

Ideally, the 2D spectrum would display two distinct peak areas, which would correspond to sites of B3 in a ring and B3 not in a ring. The isotropic projection along the diagonal of such a spectrum would produce a 1D line spectrum with quadrupolar broadening removed, as is the point of the MQMAS experiment. The peak areas in the acquired spectrum, however, are not sufficiently distinct to extract useful information about the B3 sites.

Dr Ivan Hung, University of Warwick, advised that the pulse sequence employed in the MQMAS experiments was not quite correct. This, combined with the NMR probe being perhaps not powerful enough for the purposes of this experiment, produced distorted results. It might be possible to reduce the distortion with shearing, but such processing is not simple; the correct split-t1 pulse sequence described by Brown and Wimperis[8] would have avoided the need for shearing.

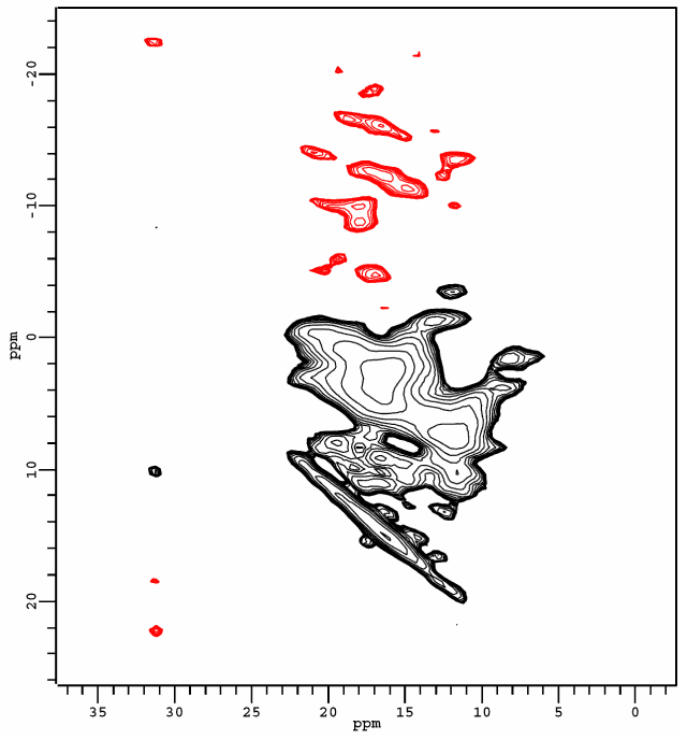

Fig. 7.

The 2D spectrum acquired from the MQMAS experiment with the x = 0 mol % lithium borate glass, after appropriate processing.

Red areas indicate negative values; black areas indicate positive values (peaks).

6.2. Raman

Fig. 6 shows the Raman spectra obtained from the lithium borate glasses. The interesting spectrum features appear between roughly 400 and 1600^{cm-1}.

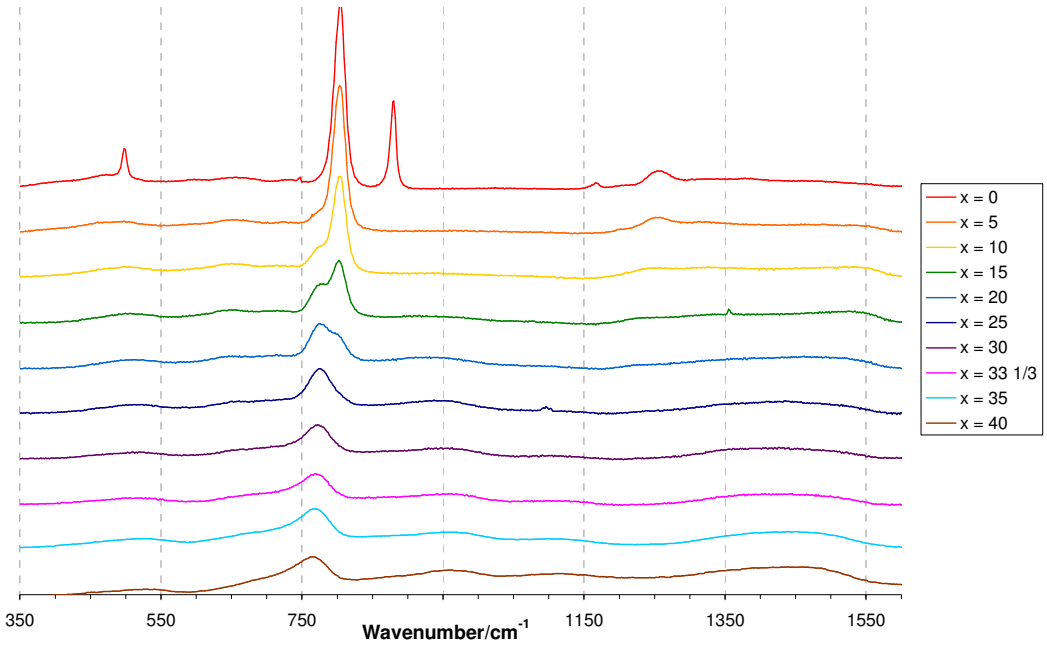

Fig. 8.

A stacked plot of the Raman spectra obtained from the lithium borate glasses.

The peak fitting for the Raman spectra was carried out, as described in section 5.3.2., and their integrated areas were found. See fig. 8 for a sample peak fitting. Trends in the areas as they changed with composition were considered, and tentative assignments of structural units to peaks were made by referring to the literature. The N4 fractions for these structural units were calculated. Combined, the peak areas, unit-to-peak assignments and unit N4 fractions allowed a plot of overall N4 fraction against composition according to Raman to be produced.

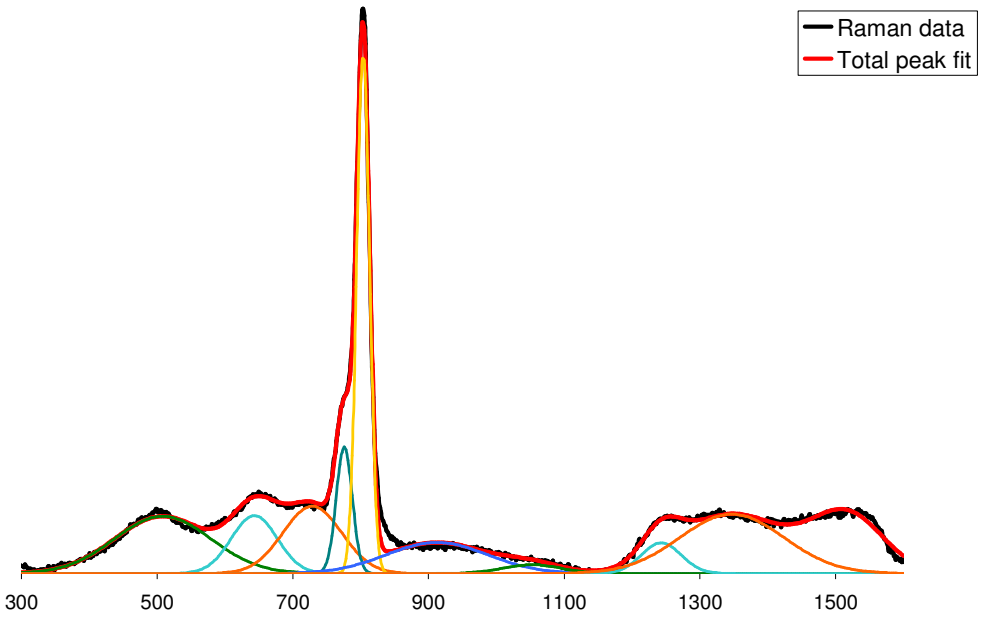

Fig. 9.

A sampled peak fit, carried out in Origin (here x = 10 mol %). The black line represents the actual Raman data; the red line represents the sum of the various peaks.

Three peaks whose areas displayed strong trends and whose unit assignments had the strongest support in the literature were selected (see fig. 9), and the peaks whose areas were roughly constant or suggested a physically unlikely trend were discarded. Attempts to make use of more (or all) the peak areas and assignments produced N4 fraction plots so far from the largely straight line obtained from corresponding NMR data that they were considered unlikely to be realistic. The discarded peak area information is a reflection of the difficulties with peak fitting the Raman spectra. The three peaks which were finally selected for use originally had the clearest locations and strongest trends, making them easier to fit.

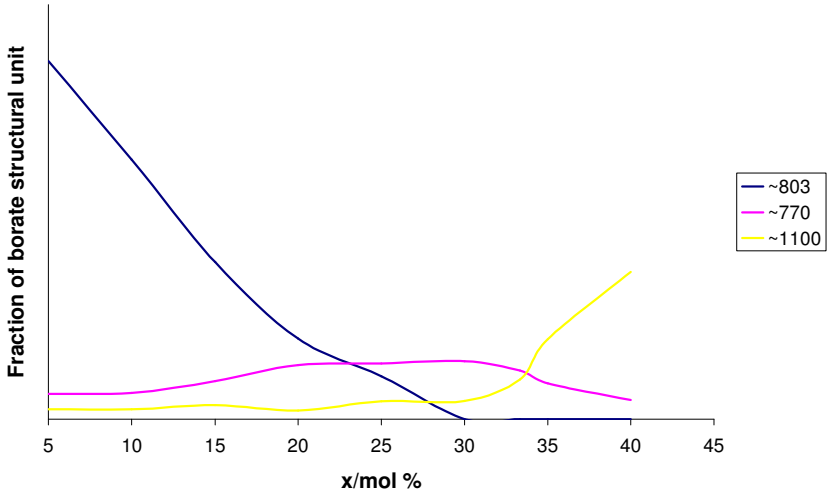

Fig. 10.

A plot of the proportional presence of selected structural units, identified by their rough location in the Raman spectra, against composition.

The peak at around 803cm^{-1} was assigned to the boroxol ring; that at 770^{-1} to the triborate group; and that at 1100^{-1} to the diborate group.

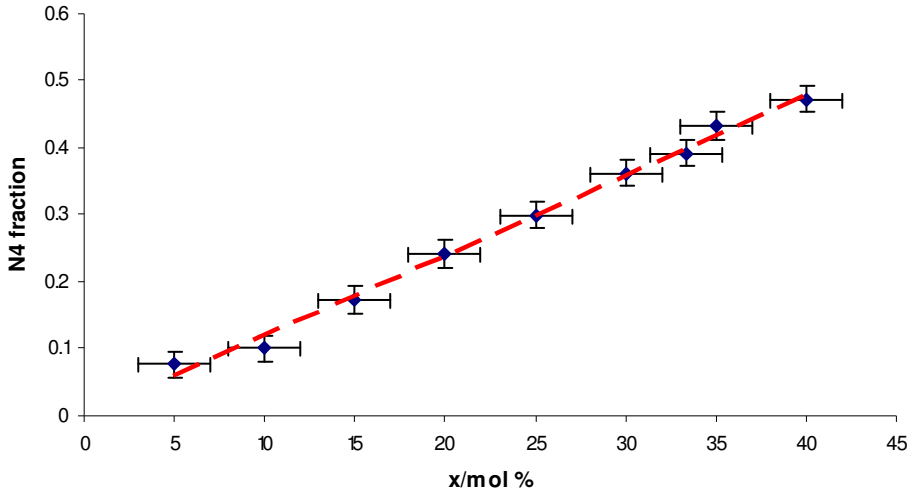

Fig. 11.

N4, the fraction of 4-coordinated boron, against composition for the lithium borate glasses, extracted from Raman data. A straight line fits the data points well; the points do not clearly suggest the levelling off after x = 30 mol % that is clear in the NMR results (see fig. 4).

Fig. 10 is the plot of N4 fraction against composition subsequently obtained. X-axis error bars were again drawn from compositional uncertainty. Error bars in the y-axis were estimated from Raman data resolution and uncertainty in Raman spectra peak fitting; the latter was the dominant source of error, though improved resolution spectra might make the peak fitting less ambiguous.

7. DISCUSSION

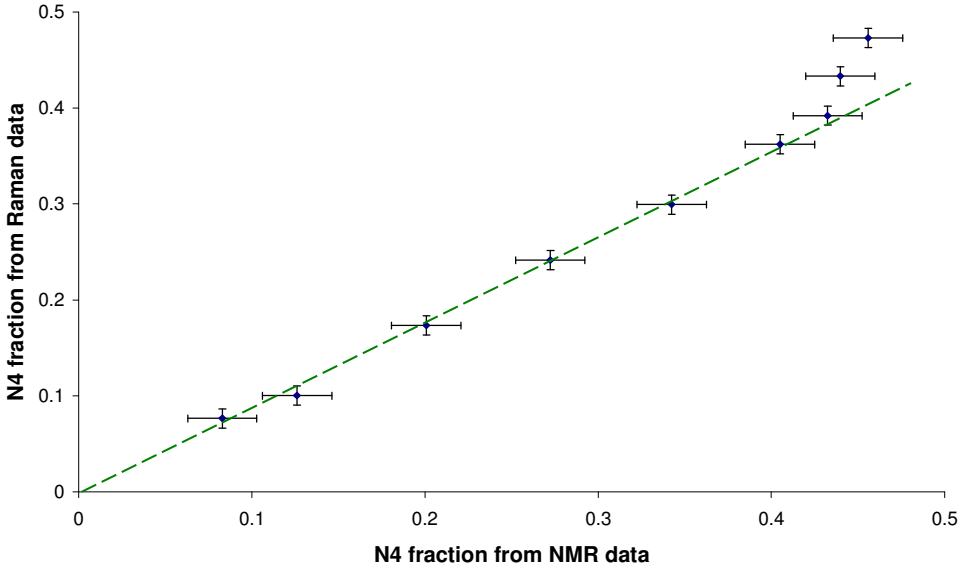

Fig. 12.

The N4 fraction results from Raman data plotted against the N4 fractions from NMR data, such that the first point corresponds to x = 5 mol %, etc.

8. CONCLUSIONS

9. REFERENCES

[1] W. H. Zachariasen, *J. Am. Chem. Soc.*, 1932, **54**, 3841-51
[2] A. C. Wright, N. M. Vedishcheva and B. A. Shakhmatkin, *Structure and Dynamics of Glasses and Glass Formers, MRS symposium* 1997, 381-96
[3] A. C. Hannon, D. Holland, *Phys. Chem. Glasses*, 2005 (.....)
[4] G. E. Jellison, S. A. Feller and P. J. Bray, *Phys. Chem. Glasses*, 1978, **19**, 52-3
[5] S. Kroeker, S. A. Feller, M. Affatigato, C. P. O'Brien, W. J. Clarida, M. Kodama, *Phys. Chem. Glasses*, 2003, **44** (2), 54-8

[6] L. van Wüllen and W. Müller-Warmuth, *Solid State Nuclear Magnetic Resonance*, 1993, **2**, 279-84
[7] A. Medek and L. Frydman, *J. Braz. Chem. Soc.*, 1999, **10** (4), 263-77
[8] S. P. Brown and S. Wimperis, *J. Magnetic Resonance*, 1997, **124**, 279-85
[9] J. F. Stebbins, P. Zhao and S. Kroeker, *Solid State Nuclear Magnetic Resonance,* 2000, **16**, 9-19
[10] B. N. Meera and J. Ramakrishna, *J. Non-Cryst. Solids*, 1993, **159**, 1-21
[11] B. P. Dwivedi, M. H. Rahman, Y. Kumar and B. N. Khanna, *J. Phys. Chem. Solids*, 1993, **54** (5), 621-8
[12] E. I. Kamitsos, M. A. Karakassides and G. D. Chryssikos, *Phys. Chem. Glasses*, 1989, **30** (6), 229-34
[13] W. L. Konijnendijk and J. M. Stevels, *J. Non-Cryst. Solids*, 1975, **18**, 307-31
[14] J.L. Shaw, A.C. Wright, R. N. Sinclair, J. R. Frueh, R. B. Williams, N.D. Nelson, M. Affatigato, S. A. Feller, C. R. Scales, *Phys. Chem. Glasses*, 2003, **44** (3), 256-9
[15] M. Affatigato, S. Feller, E. J. Shaw, D. Feil, B. Teoh, O. Mathews, *Phys. Chem. Glasses*, 1990, **31** (1), 19-24
[16] D. Massiot, F. Fayon, M. Capron, I. King, S. Le Calvé, B. Alonso, J-O. Durand, B. Bujoli, Z. Gan, G. Hoatson, *Magnetic Resonance in Chemistry*, 2002, **40**, 70-76
[17] K. J. D. Mackenzie and M. E. Smith, Multilinear Solid-state NMR of Inorganic Materials, *Pergamon Materials* Series, 6, Pergamon-Elsevier, Oxford, 2002

10. BIBLIOGRAPHY

M. H. Levitt, *Spin Dynamics*, *Basics of Nuclear Magnetic Resonance*, Wiley, 2001